Cancer Chemother Pharmacol (2008) 61:395–405
DOI 10.1007/s00280-007-0482-z

ORIGINAL ARTICLE

A new liposomal formulation of Gemcitabine is active in an orthotopic mouse model of pancreatic cancer accessible to bioluminescence imaging

C. Bornmann · R. Graeser · N. Esser · V. Ziroli · P. Jantscheff · T. Keck · C. Unger · U. T. Hopt · U. Adam · C. Schaechtele · U. Massing · E. von Dobschuetz

Received: 21 December 2006 / Accepted: 16 March 2007 / Published online: 7 June 2007

Abstract Despite its rapid enzymatic inactivation and therefore limited activity in vivo, Gemcitabine is the standard drug for pancreatic cancer treatment. To protect the drug, and achieve passive tumor targeting, we developed a liposomal formulation of Gemcitabine, GemLip (Ø: 36 nm: 47% entrapment). Its anti-tumoral activity was tested on MIA PaCa-2 cells growing orthotopically in nude mice. Bioluminescence measurement mediated by the stable integration of the luciferase gene was employed to randomize the mice, and monitor tumor growth. GemLip (4 and 8 mg/kg), Gemcitabine (240 mg/kg), and empty liposomes (equivalent to 8 mg/kg GemLip) were injected intravenously once weekly for 5 weeks. GemLip (8 mg/kg) stopped tumor growth, as measured via in vivo bioluminescence, reducing the primary tumor size by 68% (SD ± 8%; $p < 0.02$), whereas Gemcitabine hardly affected tumor size (-7%; ± 1.5%). In 80% of animals, luciferase activity in the liver indicated the presence of metastases. All treatments, including the empty liposomes, reduced the metastatic burden. Thus, GemLip shows promising antitumoral activity in this model. Surprisingly, empty liposomes attenuate the spread of metastases similar to Gemcitabine and GemLip. Further, luciferase marked tumor cells are a powerful tool to observe tumor growth in vivo, and to detect and quantify metastases.

Keywords Liposomes · Gemcitabine · Orthotopic · Bioluminescence · Pancreatic cancer

C. Bornmann and R. Graeser have equally contributed to this article.

C. Bornmann · T. Keck · U. T. Hopt · U. Adam · E. von Dobschuetz
Department of General and Visceral Surgery,
Albert-Ludwigs-University Freiburg, Freiburg, Germany

R. Graeser (✉) · N. Esser · C. Schaechtele
ProQinase GmbH, Breisacher Strasse 117,
79106 Freiburg, Germany
e-mail: r.graeser@proqinase.com

V. Ziroli · P. Jantscheff · C. Unger · U. Massing
Tumor Biology Center, Freiburg, Germany

Introduction

With around 2% of all cases in the USA, pancreatic cancer is among the ten most frequent, but within the top five mortal cancers (5% of total). At present, the only potentially successful treatment is the surgical removal of the primary tumor, but due to its very early invasion of the surrounding tissue and organs, the recurrence rate is extremely high. Thus, pancreatic cancer has a very poor prognosis. It is estimated that less than 4% of all patients suffering from pancreatic cancer will survive longer than 5 years after diagnosis [1].

Chemotherapy of pancreatic cancer is, at present, only a palliative treatment. The drug of choice is Gemcitabine [2], a nucleoside analogue, which, compared to the former standard drug 5-fluorouracil, shows a slightly increased response rate and median survival of the patients. The rather limited activity of Gemcitabine in treating pancreatic cancer is surprising, considering the in vitro sensitivity of pancreatic cancer cells to the drug with LD_{50}'s in the lower nM-range [3, 4].

One explanation for the low systemic activity of Gemcitabine is its very short half-life of 8–17 min in human plasma [5–7] and about 9 min in murine plasma [8]. In plasma, deaminases rapidly convert Gemcitabine to its inactive metabolite, dFdU [5–7]. Within tissues, its half-life is somewhat extended. Radio-labelled Gemcitabine remained up to 3 h in normal mouse tissues, as well as in soft tissue sarcomas growing subcutaneously in mice [8, 9]. However, since total radioactivity was quantified in these

studies, it was not possible to distinguish Gemcitabine from its inactive metabolite, dFdU.

Entrapment of drugs in liposomes may provide protection from rapid metabolic inactivation [8, 10, 11]. Moreover, entrapment of Gemcitabine within liposomes might mediate passive tumor targeting by the so called enhanced permeability and retention (EPR)-effect. The, compared to healthy tissues, more leaky vasculature of tumors and metastases [12–14] allows extravasation of small liposomes (<200 nm) into the tumor and their accumulation therein.

However, Gemcitabine at physiologic pH is an uncharged, low-molecular weight molecule, which readily diffuses through liposome bilayers. Entrapment of Gemcitabine into a vesicular phospholipid gel (VPG) by the passive loading technique [15] resulted in a formulation in which the drug is equally distributed over the whole VPG. Equal concentrations of Gemcitabine inside and outside the liposomes prevent the formation of a gradient, and the ratio of Gemcitabine between the vesicle cores and the aqueous space remains constant. The formulation used in this study was thus stable for more than three months at 4°C in terms of Gemcitabine- and phosphatidylcholine-content, as well as particle size.

In a previous study, using mice-bearing soft tissue sarcomas, the plasma half-life of Gemcitabine entrapped in VPGs was extended to 13 h, resulting in a 35-fold higher area under the curve, and a drop of the maximal tolerable dose (MTD) from 360 mg/kg down to 6–9 mg/kg. The accumulation of entrapped Gemcitabine in the tumor—as measured using radio-labeled Gemcitabine—was increased by a factor of 4, and was accompanied by a threefold to fourfold increase of its half-life within the tumor to ca. 10 h [8]. Taking into account that the increased radioactivity was mainly attributable to liposomal Gemcitabine, and its protection from degradation to dFdU, one might assume that the net increase of intact Gemcitabine was actually much higher than the four times determined. Indeed, GemLip, at 8 mg/kg, showed better activity than the free drug at MTD, and complete remissions were observed. In an orthotopic bladder cancer mouse model, the anti-tumoral activity of GemLip was confirmed, and found to be superior to that of paclitaxel or vincristine. Furthermore, none of the animals treated with GemLip showed any detectable metastases [16].

In the above mentioned studies, a GemLip formulation with an average liposome size of about 60 nm and an entrapping efficiency of 33% was used. In the present study, the liposome size was decreased to 36 nm, with an entrapment efficiency of 47%. The smaller particle size may improve the diffusion from the blood stream into the tumor and metastases, and thus increase the targeting efficiency. Furthermore, the present formulation allowed GLP-like production, therefore, if equally successful, facilitating its use in patients.

To test this improved formulation of GemLip, we chose the pancreatic cancer cell line MIA PaCa-2, a poorly differentiated pancreatic ductal carcinoma cell line [17] that is widely used for drug treatment studies, and is very sensitive to Gemcitabine [18]. If implanted orthotopically into the pancreata of nude mice, the MIA PaCa-2 cell line metastasizes locally to the intestine, spleen and liver, but also, albeit rarely, to the lung [19, 20]. Two methods have been described to orthotopically implant MIA-PaCa2 cells, either involving a direct injection of tumor cells into the pancreas [21, 22], or the implantation of pieces of a subcutaneously grown tumor [19, 23]. Since a spilling of cells during the injection process may generate artificial metastases, the route via subcutaneous implantation of tumor cells was chosen.

Other than from subcutaneously injected cells, tumors developing from orthotopically implanted cells are not easily palpable. To allow randomization of the animals at the onset of the treatment, and to exclude non-tumor-bearing animals, as well as to monitor drug effects during the treatment period, the MIA PaCa-2 cells used in this study were marked with luciferase. The light emission of such cells can be detected in vivo using a CCD camera after injection of luciferin i.p. into the mouse [24]. The use of the light emitting luciferin/luciferase system was chosen rather than GFP or RFP labeling due to the improved signal to noise ratio, and the possibility to quantify tumor and metastases burden via enzymatic luciferase assays at the time of necropsy.

The aim of this study was to compare the anti-tumoral and anti-metastatic activity of free Gemcitabine with that of the improved VPG encapsulated formulation of Gemcitabine (GemLip) in our orthotopic pancreas model. During the treatment, tumor sizes were measured weekly using bioluminescence in vivo imaging. Tumor sizes, as well as luciferase activity from potential target sites for metastases were determined as endpoints.

Materials and methods

Preparation of Gemcitabine liposomes (GemLip)

Vesicular phospholipid gels consisted of hydrogenated egg phosphatidylcholine/cholesterol (55:45 molar ratio; Lipoid AG, Ludwigshafen, Germany) at a total lipid concentration of 40% (w/w) (660 mM lipid). For each batch of VPG, 12 g lipid mixture was hydrated with 18 ml mannitol solution (5%), and treated with a high pressure homogenizer (Micron Lab 40, 70 Mpa, 10 cycles; APV Gaulin, Lübeck, Germany). The resulting "empty VPG" were aliquoted into 30 ml injection vials (Zscheile & Klinger, Hamburg, Germany) in portions of 3.71 g. 6 g glass beads (5 mm in diameter) were added as shaking aid, the vials were closed with

a silicone rubber stopper, autoclaved at 121°C, 2 bar, 20 min. and stored at 4–8°C [25].

For the entrapment of Gemcitabine (Gemzar®; kindly provided by Lilly-Deutschland GmbH Bad Homburg, Germany) within the empty VPG, the "passive loading" technique was employed [15]. In short, 0.5 ml Gemcitabine solution (38 mg/ml in 0.9% NaCl) was added to the VPG containing vials, the components were thoroughly mixed using a microdismembrator (1,500 shakes/min, 10 min), incubated for 1 h at room temperature and mixed a second time (1,500 shakes/min, 5 min.). To ease the diffusion of Gemcitabine into the liposomes, the mixtures were incubated at 60°C for 2 h in an aluminium block. Final Gemcitabine conc. in the dual formulation is 19 mg/vial.

GemLip-VPG was dispersed with 6.4 ml of a 0.9% sterile NaCl solution to yield a final total lipid concentration of 231 mM, and mixed (1,500 rpm, 10 min.). The resulting GemLip was pushed through a 5 µm particle filter (Braun Melsungen AG, Melsungen, Germany) and further diluted for the animal injections.

Liposomal Gemcitabine-content was analyzed using HPLC [8]. For this purpose, non-entrapped Gemcitabine was removed from the liposomal dispersion by adsorption over a cationic exchange resin AG 50W X-8 (Bio-Rad, Munich, Germany) activated with conc. NaCl.

Generation of luciferase expressing MIA PaCa-2 cells

The retrovirus encoding the luciferase–aminoglycoside phosphotransferase (Neomycin resistance) fusion gene (Luci–Neo) was constructed from the luciferase gene of pUHC 13-3 (pTRE Luc [26]), and the neomycin resistance gene from pcDNA 3.1 (Invitrogen), using pLib (BD Clontech) as a backbone. The EF1α promoter was derived from a pEF vector (Invitrogen), and introduced upstream of the Luci–Neo fusion gene. The transduction of the MIA PaCa-2 (ATCC #CRL-1420) cells using a VSV-G (BD Clontech) pseudotyped retrovirus was performed according to the instructions from the manufacturer. After selecting successfully transduced cells using 1–3 mg/ml Neomycin, their luciferase activity was tested. 10^6 cells were lysed in 100 µl in 1 × luciferase lysis buffer (25 mM TRIS–phosphate pH 7.8; 2 mM EDTA; 2 mM DTT; 0.1% Triton X-100), the lysate was serially diluted, and assayed for luciferase activity (Promega E4550), according to the manufacturer's instructions in a Luminometer (BMG Lumistar).

Determining the IC_{50} of MIA PaCa-2 to Gemcitabine and GemLip

One hundred microliter of the cells were seeded at 2×10^5/ml per well into a 96 well plate. After 24 h, Gemcitabine and GemLip were added at indicated concentrations and the cells were incubated for another 48 h. Four hours before lysis, the BrdU reagent (Roche, Diagnostics GmbH, Penzberg, Germany) was added for 4 h. Culture supernatants were removed, the cells were fix-dried for 1 h at 60°, and stored at 4°C. BrdU assays were performed according to the manufacturer's instructions.

Animal experiments

All animal experiments were performed in accordance to German Animal License Regulations (Tierschutzgesetz) identical to UKCCCR Guidelines for the welfare of animals in experimental neoplasia [27]. Female athymic Nude (Hsd:Athymic Nude-Foxn1nu) mice were obtained from Harlan Winkelmann GmbH, Germany.

To produce the MIA PaCa-2 donor tumors, 5×10^6 cells per animal in 100 µl PBS were injected subcutaneously into the left flank of a nude mouse. Tumor sizes were measured three times weekly via callipering.

At a size of 0.5–1 cm^3, subcutaneously grown tumors were aseptically removed from donor animals, and transferred into Petri dishes containing 10 ml of pre-warmed tissue culture medium. Macroscopically vital areas of the tumor were cut into 1 mm^3 pieces using a scalpel. Mice were then anesthetized with isofluorane, and the abdomen was sterilized with alcohol. An incision was made along the backside of the spleen, and the pancreas was carefully exposed. A pocket of 2–3 mm was prepared in the pancreas tail, using the major spleen vein as a leading structure, and the tumor pieces were inserted. The pancreas was then re-inserted into the abdomen, and the abdominal wall was closed using 5-0 Dexon sutures (DEXON®, B.Braun-Dexon, Spangenberg, Germany).

Analysis of tumor permeability (Evans Blue assay)

Mice were injected 100 mg/kg of Evans blue (10 mg/ml in 0.9% NaCl). After 30 min, the mice were sacrificed, blood samples as well as samples from tumor and skeletal muscle were taken, weighed and homogenized in 1/9 parts (w/w) of an 0.1% sodium sulfate/aceton mixture (7:3 v/v). After 17 h incubation at room temperature in the dark, the samples were centrifuged at 1,000*g* for 5 min. The absorbance of each supernatant was determined at 620 nm, and the concentration of Evans blue was quantified by comparing to a standard. The amounts of Evans blue in the tumor tissue and skeletal muscle were calculated per tissue weight, and standardized for the measured blood concentration.

Measurement of in vivo bioluminescence

The animals were anesthetized via intra-peritoneal (i.p.) injection of a mix of 15 µl Domitor® (10 mg/kg; Pfizer) and

20 µl Ketamin (20 mg/kg; Essex Tierarznei). One hundred microliter of the substrate, D-Luciferin (20 mg/ml; Molecular Imaging Products, Ann Arbor, MI, USA), were then injected i.p., and the animals were left for 10 min on a cushion heated to 37°C. Before exposing the animals to the camera (CCD-camera LNU/S, PerkinElmer), the eyes were treated with Oculotect® (Novartis), to prevent blindness caused by corneal dryness. Animals bearing subcutaneous tumors were exposed for 1 sec, those with orthotopically implanted tumors 5 min. The waking-up period was shortened by injection of 50 mg/kg Antisedan® (Pfizer). Raw, unmodified images from the camera were imported into Adobe Photoshop 7.0® and transformed to 8-bit indexed color format. To help visualizing the primary tumor, levels were set to 0–25, and the color table 'spectrum' was applied (the latter two steps did not change the information content of the files, only helped to localize the signal for the graphical quantification in ImageJ). The files were then opened in imageJ, and the mean pixel intensity of 150 pixel squares drawn at the site of the primary tumor was measured, and the results were used to generate growth curves.

Necropsy and luciferase assays of mouse organs

Mice were sacrificed, the abdominal cavity was opened, and a picture of the tumor in situ was taken. The primary tumor was then resected, measured, and its volume was calculated using the formula $V = a^2 \times A/2$ (a—small diameter, A—large diameter). It was then weighed, and cut in two pieces. One was shock frozen in liquid nitrogen for histology, the other homogenized in 2 ml of luciferase lysis buffer. To get a quantitative analyse of the metastatic spread into potential target organs, the liver, spleen, and lungs were resected from the animals, taking great care to prevent cross-contamination of the tissues. Whereas part of these organs were also cryo-preserved, samples from the intestine, the stomach, as well as inguinal lymph nodes and 'normal' pancreatic tissue were only analysed in luciferase assays. After homogenization, insoluble material was spun 10′ at 3,000 rpm in a Heraeus Megafuge 2.0. 5 µl were checked for protein concentration using a Bradford assay (Sigma B6916) with BSA serving as a standard protein, and 10 µl were measured in a luciferase assay (Promega E4550).

Histology

Seven micrometer cryo-sections were prepared, and either processed for immunohistochemistry, or assayed for luciferase activity, followed by H&E staining. For the former, the sections were fixed using 4% paraformaldehyde and stained for human cytokeratin using the biotinylated mouse monoclonal pan cytokeratin 1–8 antibody from Progen (Cat # 61506) according to the instructions from the manufacturer. In the latter case, the sections were overlaid with a luciferase substrate mix (Promega E4550), exposed under a Nightowl camera (Berthold) for 2 min. at 1 × 1 binning, washed in water, and stained H&E to reveal the morphology of the sections.

Results

Generation and characterization of MIA PaCa-2 cells expressing luciferase

The luciferase gene was transduced into MIA PaCa-2 cells with a retrovirus encoding a luciferase-neomycin (LN) resistance fusion protein. The expression of the fusion gene is driven either by the retroviral LTR (LN) or by an inserted additional EF1α promoter (ELN). Successfully transduced cells were selected using neomycine, and the resulting cell pools checked for the expression of luciferase in an in vitro luciferase assay. To prevent the generation of clonal artefacts, we decided to use cell pools rather than a cloned cell line. The use of a luciferase–neomycin resistance fusion protein prevents the generation of false positive cells.

The luciferase activity of the MIA PaCa-2 LN cell pool was 50 ± 8 LU/cell, that of the MIA PaCa-2 ELN cell pool 70 ± 10 LU/cell (Fig. 1a). This level of luciferase expression remained constant even if Neomycin was omitted from the medium, and was slightly above the average obtained from the cell lines transduced with these vectors so far (data not shown). Although a robust in vivo signal would be expected from either of the cell lines, the MIA PaCa-2 ELN cells were chosen for further experiments, since their luciferase activity was slightly higher than that of the LN cells.

Next, we checked whether the transduction process may have altered the proliferation rate, or the sensitivity of the cell line to Gemcitabine. No difference in the proliferation rate of the two cell lines in the untreated culture was found (Fig. 1b). Also the IC_{50} values for Gemcitabine, 8 nM (parental), and 19.4 nM (ELN), were in the same order of magnitude (Fig. 1b), and within the range of previously reported values for MIA-PaCa2 [4, 18, 28]. The liposomal formulation of Gemcitabine displayed similar activity in vitro to that of the free drug (Fig. 1b).

Thus, the cell lines were sensitive towards the drugs, and no evidence for a transduction mediated alteration in growth behaviour, or drug sensitivity, of the recombinant luciferase expressing MIA PaCa-2 ELN was discovered.

Subcutaneous implantation of parental and ELN MIA PaCa-2 cells in nude mice

To prevent an artificial dissemination of the tumor cells when implanted orthotopically, we decided to implant

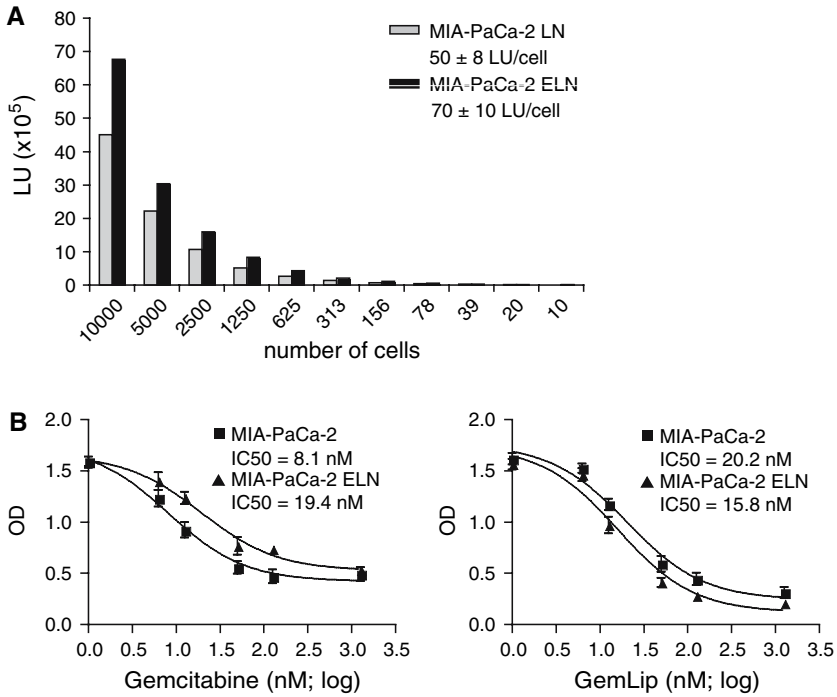

Fig. 1 In vitro characterization of MIA PaCa-2 cells expressing luciferase. **a** In vitro luciferase assay. To compare the luciferase expression of the MIA PaCa-2 LN and ELN cells, 10^6 cells were lysed in 100 µl luciferase lysis buffer, and 10 µl of the lysate (10^5 cells) were diluted in 90 µl of buffer. From this, a series of 1/2 dilutions down to 100 cells per 100 µl was prepared, and 10 µl of each dilution were used to measure luciferase activity. A *bar graph* indicating the light units (*LU*) emitted is shown. **b** Sensitivity of parental and transduced cells to Gemcitabine and GemLip. Parental MIA PaCa-2 and MIA PaCa-2 ELN were plated in 96 well plates. Gemcitabine, or GemLip, was added 24 h later at the indicated concentrations, and the cells were incubated for an additional 48 h. Four hours before lysis, BrdU was added. BrdU incorporated into the genomic DNA was then quantified via ELISA

pieces from a subcutaneously grown tumor, rather than to inject a cell suspension. To generate the donor tumors, the MIA PaCa-2 ELN cell line was injected subcutaneously into NMRI mice, alongside with the parental cell line, which served as a control for the in vivo growth behaviour of the transduced cell line.

Both subcutaneously injected cell lines formed tumors with a 100% take rate and comparable growth (Fig. 2a). Within 30 days, the tumors reached a size of ca. 1 cm^3 (Fig. 2a), and were ready for orthotopic implantation. The MIA PaCa-2 ELN tumors were checked for luciferase activity before resection, and revealed a strong bioluminescence signal (data not shown).

Orthotopic implantation of MIA PaCa-2 ELN cells

Viable areas of the subcutaneously grown MIA PaCa-2 ELN tumors were cut into pieces of 1 mm^3 and inserted into the tail of the pancreas of nude mice. The success of the procedure was controlled 7 and 14 days after the surgical operation via measurement of the luciferase activity of the implanted tumor pieces. After 7 days, 90% of the mice showed a signal in the region of the pancreas, at day 14, the rate had increased to 93% (51/55 mice with a detectable signal).

Tumor vessel permeability

The passive targeting of liposomes is mediated mainly by the enhanced vascular permeability of the tumor vessels. To measure the vascular permeability of our orthotopically implanted MIA PaCa-2 tumors, three tumor bearing mice were intravenously (i.v.) injected with Evans Blue, which binds to serum albumin, and thus accumulates in tissues with leaky vasculature. Indeed, the vascular permeability was found to be nearly five times higher in tumor tissue than in the reference skeletal muscle (see Fig. 2b).

Treatment with Gemcitabine/GemLip

Two weeks after implantation, the animals were assigned to treatment groups of ten each. Quantification of the light emission by the tumors was used as a proxy to randomize the animals according to the tumor sizes (Fig. 3a). At that time, the tumors were not yet palpable.

The drugs were applied i.v. once weekly, Gemcitabine at 240 mg/kg, GemLip at two dosages, 4 and 8 mg/kg, and, as a control, empty liposomes at a dosage corresponding to the 8 mg/kg GemLip. Although a 3-days schedule using 120 mg/kg was reported as the most effective schedule for

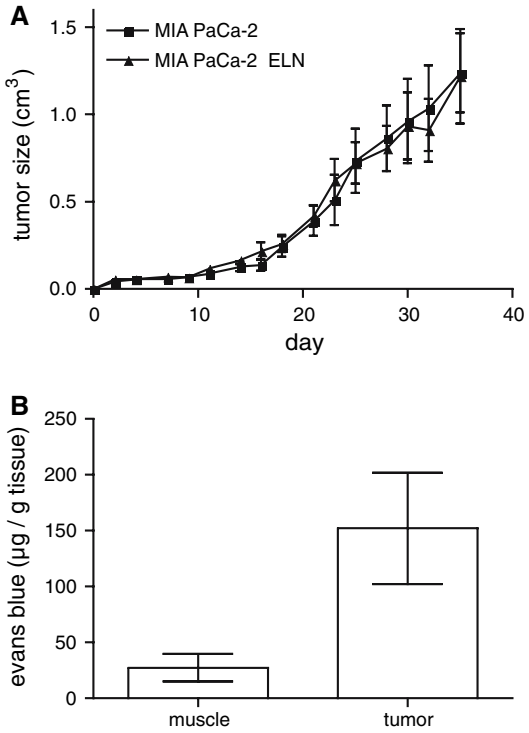

Fig. 2 In vivo characterization of MIA PaCa-2 ELN. **a** Comparison of the in vivo growth characteristics of parental and MIA PaCa-2 ELN cell lines in NMRI mice. 2×10^6 cells were injected subcutaneously into NMRI mice, and the growth of the tumors was monitored via callipering three times per week. A growth curve using the mean values for each group ($n = 4$) and time-point is shown. The *error bars* represent the SEM. **b** Evans blue staining of mice to determine tumor vessel leakiness. Mice were injected 100 mg/kg of Evans blue. After 30 min, the mice were sacrificed, and blood samples as well as samples from tumor and skeletal muscle tissue were removed. The dye was solubilized as described in Materials and methods. The concentration of Evans blue was then determined spectro-photometrically, adjusted for each mouse to the concentration in the blood, and the total amount in the samples investigated was calculated. A *bar graph* representing the mean weight of Evans blue per gram tissue in the respective sample, and the SEM for each group ($n = 3$) is shown

Gemcitabine [29], a weekly schedule was chosen here in order to be able to compare the results with the weekly schedule of GemLip. A 3-days schedule for GemLip was not recommended due to its extended half-life [8]. Since the half-life of GemLip predominantly depends on the elimination of its liposomal carrier, the increased dosage of liposomes used here would be expected to result in an even more pronounced extension of its half-life [14]. During the treatment period, tumor sizes were monitored once weekly by luciferase measurements, as well as the animals' body weights three times weekly as indicator of their health status. After 5 weeks, the animals were sacrificed, and tumor size and weight, as well as luciferase activities of potential target organs for metastases were determined.

No weight losses were observed in any of the treatment groups, indicating that the treatments were well tolerated (data not shown). Control tumor values increased regularly, except for the last measurement. The reason for the drop at the last time-point is not really clear (Fig. 3b, squares, as well as panel to the right). However, such variations between the weekly measurements were observed occasionally (e.g. Fig. 3c control day 21; Fig. 3b, Gemcitabine treatment group, 21 days vs. 28 days measurement), and, unless significant, were usually found to be reversed at the next time-point.

Using the above described weekly schedule, free Gemcitabine (240 mg/kg), did not have an effect on the growth of the tumors (Fig. 3b, triangles). Neither did GemLip at the lower dosage of 4 mg/kg (Fig. 3b, inversed triangles), or the empty liposomes (Fig. 3b, circles). However, treatment with GemLip at a dosage of 8 mg/kg resulted in a clear reduction of tumor growth during three consecutive weeks of treatment (Fig. 3b, diamonds; right panel; single animals control vs. 8 mg/kg GemLip in Fig. 3c).

Analysis of drug effects on the primary tumor (endpoint)

After the 5 weeks treatment period, the animals were sacrificed, pictures of the primary tumor site were taken, and tumor sizes and weights were determined.

The increase of the tumor size measured via in vivo bioluminescence from day 14, when the animals were randomized, to day 48, before necropsy, was significant for all groups, except for the GemLip 8 treatment group (Fig. 4a; *P* values determined using student's *t* test). Thus GemLip at 8 mg/kg prevented the progression of tumor growth for 34 days.

The observed anti-tumoral effect of GemLip at 8 mg/kg was confirmed by measurement of the actual tumor sizes. The difference in average tumor size between the 8 mg/kg and the untreated control group was statistically significant (student's *t* test; $P = 0.019$; Fig. 4b). Furthermore, the lack of an anti-tumoral activity of the free drug in vivo was confirmed. Even if the one very large tumor in the Gemcitabine group is not taken into account (Fig. 4b, grey bar), the average tumor size does not differ significantly from the average in the control group.

Thus GemLip at 8 mg/kg, compared to an equitoxic dosis of the free drug, showed improved activity on the primary tumor in this orthotopic model for pancreatic cancer, with no apparent negative effect on the animals' welfare.

Analysis of drug effects on the metastases (endpoint)

To detect and quantify the metastatic burden of the animals, they were visually inspected for metastases first, followed by resection of potential target organs (pancreas, spleen, liver, stomach, intestine, lung, and the local lymph nodes) and performance of luciferase assays of tissue homogenates.

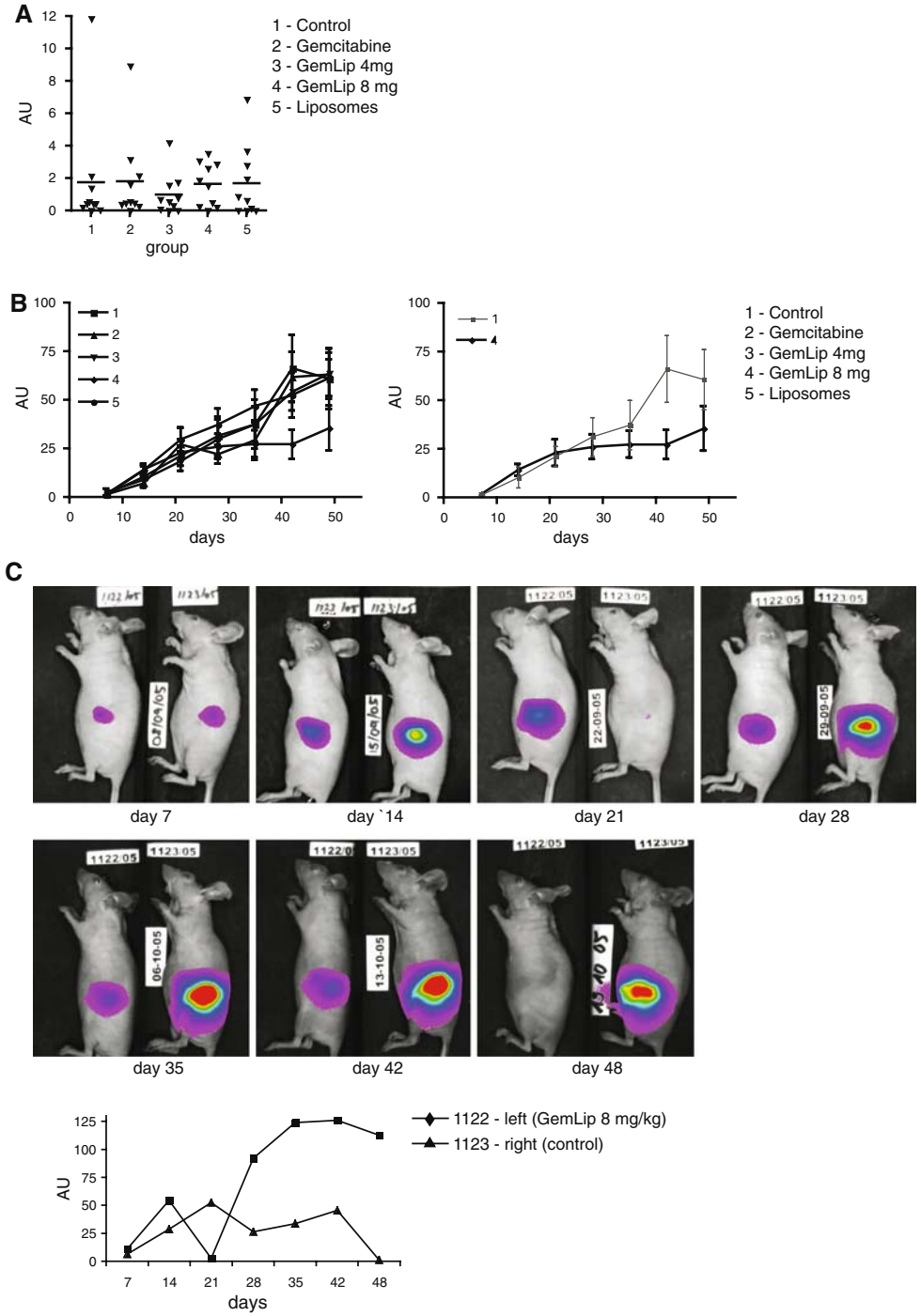

Fig. 3 Monitoring drug effects and toxicity via measuring in vivo luciferase activity of the orthotopically implanted MIA PaCa-2 ELN cells and animal weights. **a** Randomization of tumor-bearing animals 14 days after implantation. The animals were anesthetized, injected with 2 mg luciferin, and, after 10 min, the light emitted by the tumors was collected for 5 min by a CCD camera. The light emission was quantified graphically (see Materials and methods), and the animals were randomized accordingly. A *scatter graph* representing the individual values, and the mean for each group ($n = 10$) is shown (AU—arbitrary units). The mean for the 4 mg GemLip group was slightly lower, but not significantly different from the other groups. **b** *Tumor growth curve* The luciferase activity of the tumors was measured once weekly as described in Fig. 3a. A *growth curve* using the mean values for each group ($n = 10$) and time-point is shown. The *error bars* represent the SEM. The *right panel* shows the control group in comparison with the 8 mg/ml GemLip treatment group. **c** Exemplary results from in vivo luciferase measurements, quantification, and generation of *tumor growth curves*, showing one animal from the control group (*right*), and one from the 8 mg/kg GemLip group (*left*). Overlays of a picture of the mice with the light signal encoded as a spectrum with red representing the most, and blue the least intense light, are shown. The luciferase activity of the tumors was quantified graphically (see Materials and methods). Tumor end-volumes were 0.45 cm^3 (1,122), and 1.69 cm^3 (1,123), respectively

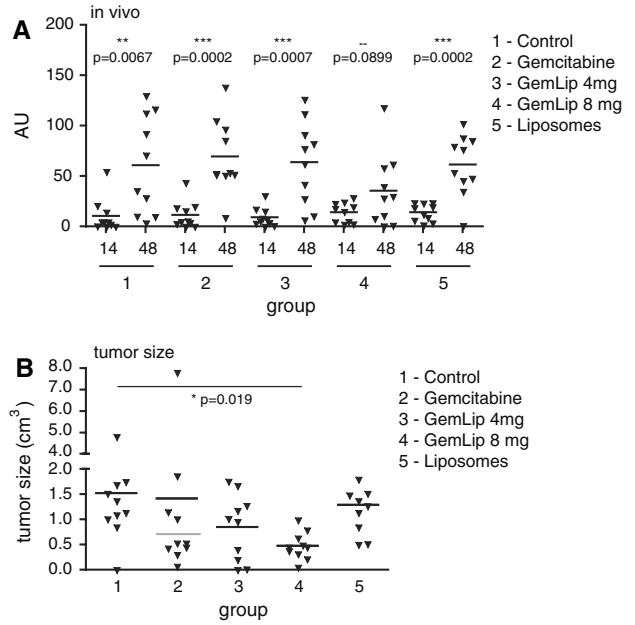

Fig. 4 Drug effects on the primary tumor (endpoint analysis). **a** A comparison of the in vivo bioluminescence activity of the tumors (as a proxy of tumor size) between the day the animals were randomized, and the day before the experiment was terminated. Tumor growth resulted in statistically significant differences in the light signals between day 14 and 48 in all groups, except of the GemLip 8 group ($n = 10$). Similar results were also found if days 14 and 42 were compared (data not shown) **b** Tumor size. Tumor sizes were measured using a calliper, and the volume was calculated. A *bar graph* representing mean and SEM for each group ($n = 10$) is shown. In order to include all tumors, the *Y*-axis was segmented. The *grey bar* in the Gemcitabine group represents the SEM excluding the one excessively big tumor

In the superficial inspection of the animals for metastases, 14 animals (28%) scored positive, mainly in the spleen (7/14%) and intestine (6/12%). Sensitive luciferase assays from organ homogenates were then used to detect, and quantify, smaller metastases, or those hidden internally. If metastases were found during the visual inspection, they generally correlated well with in vivo luciferase signals, and high scores in the respective in vitro luciferase assays (for an example, see Fig. 5a).

Overall, the liver was identified as the main target for the dissemination of metastases from the MIA PaCa-2 tumors—in 80% of the animals, luciferase activity was detected in the liver (Fig. 5b). Other organs affected were the lung (58%), the stomach (48%), and the spleen (34%). Some of the luciferase signals were rather low, indicating the presence of micro-metastases, which would explain why they remained unrecognized during the visual inspection.

A quantitative analysis of the total and liver metastases indicated that all treated animals had a reduced metastatic burden compared to the control, except for the 8 mg/kg GemLip group (Fig. 5c). The reduction was not significant, however, mainly due to the presence of animals with low metastatic counts in the control group. But, very unexpectedly, the treatment of the mice with the empty liposomes, which served as a control for the 8 mg/kg GemLip formulation, resulted in a similar reduction of metastases (Fig. 5c).

To validate the luciferase assays on tissue homogenates, frozen sections were prepared from the liver of tumor bearing animals, and luciferine and ATP were applied to identify tumor cells in the sections. The emitted light was detected using a CCD camera, and the sections were subsequently H&E stained to analyse the morphology of the positively scoring areas. Using this method, metastases could be found on the liver surface (Fig. 6a, left panel), as well as within the organ (Fig. 6a, right panel). Superficial analysis of surrounding areas did not give any evidence of additional metastatic lesions (data not shown). Thus, measuring luciferase activity in tissue homogenates provides a sensitive tool to analyse and quantify metastasizing tumor cells in organs.

If a separation of normal pancreas tissue and tumor was possible, each tissue was individually checked for luciferase activity. In only 28% of animals, the pancreas was apparently free of tumor cells, all others showed infiltration to a certain extent (Fig. 5b). The high luciferase activity may either be due to contamination with the adjacent tumor tissue, or reflect infiltration by the tumor cells. Immunohistochemistry analysis suggested that, at least to some degree, the latter was the case (Fig. 6b).

Discussion

At present, Gemcitabine is the treatment of choice for pancreatic cancer [2], although it does not lead to tumor clearance. The aim of the present study was to test whether an entrapment of Gemcitabine within liposomes, which may protect the drug from its rapid enzymatic degradation and mediate its passive accumulation within the tumor and metastases by the EPR effect, increases its activity against a model of pancreatic cancer in the mouse. The vascular permeability of the MIA PaCa-2 tumors was about fivefold higher than that of skeletal muscle used as a standard (Fig. 2b), thus allowing passive accumulation of the liposomes in the tumor. Since the liposomes used in this study were smaller than those used in a previous GemLip study [8], an even more pronounced accumulation may be expected.

Using bioluminescence as a proxy for tumor sizes allowed us to randomize the animals at the onset of the drug treatment according to their tumor sizes, as well as to exclude animals without, or with obviously misplaced tumors. Furthermore, the effect of the drug treatment on the tumor growth could be monitored, providing data on the kinetics of drug response. Occasional failures of the

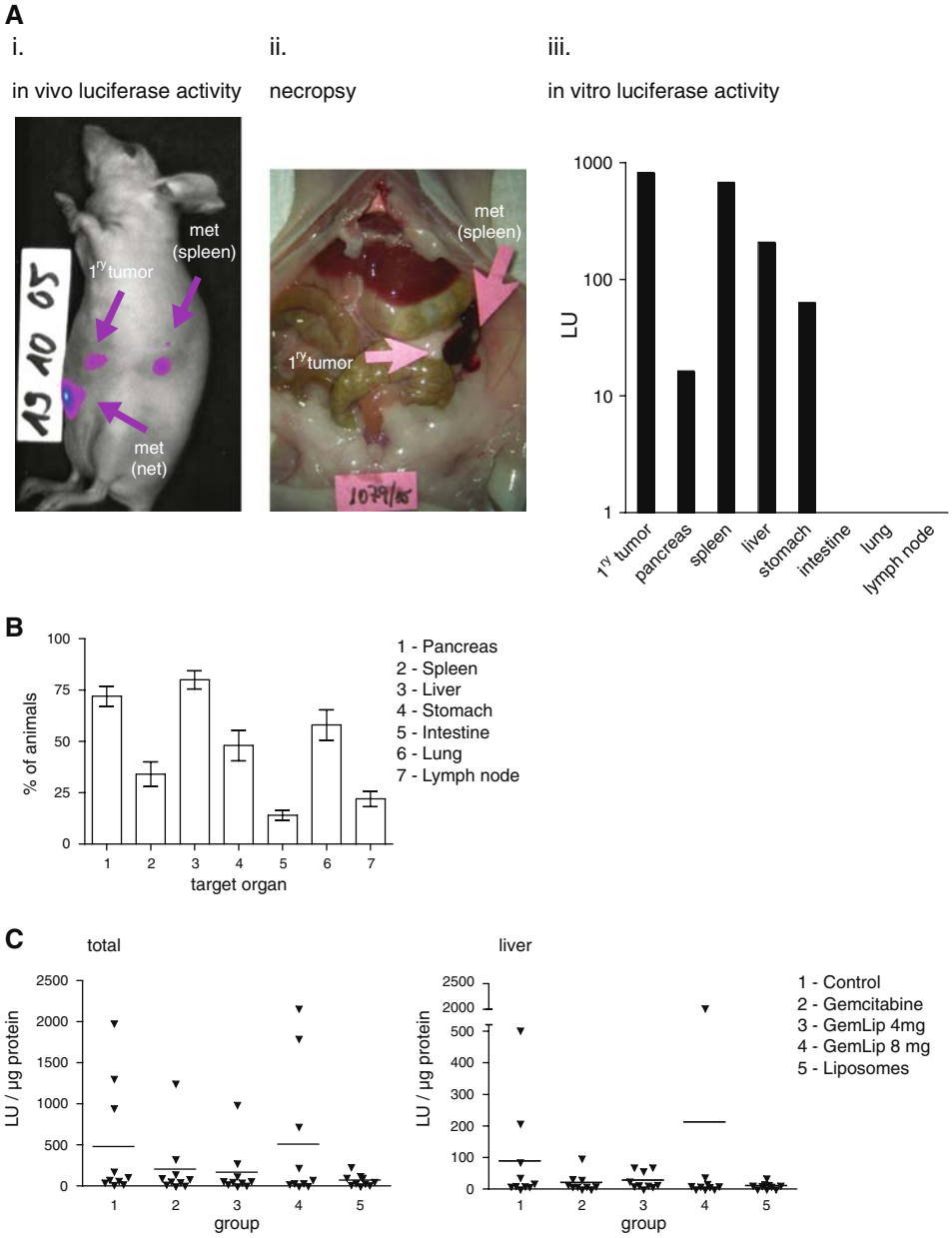

Fig. 5 Analysis of metastatic distribution and drug effects on metastasis. **a** Comparison of in vivo luciferase detection with necropsy results and in vitro luciferase activity (example) *i* In vivo luciferase activity. The picture was generated as described in Fig. 3d. The position of the primary tumor, the spleen metastasis, and a metastasis located in the net *ii* Primary tumor, and macroscopically visible metastases. After sacrificing the mouse, the abdominal cavity was opened, and a picture was taken using a digital camera. *Arrows* point at the primary tumor as well as a visible spleen metastasis. *iii* In vitro luciferase activity. A *bar graph* showing the luciferase activity detected in the organs as indicated below. Note that the tumor lysate was diluted 1/10. **b** Luciferase activity in organs. One half of potential target organs for metastases dissemination or infiltration was homogenized as described above, and the luciferase activity was determined from 10 µl of the undiluted extract. The protein concentration was determined by a Bradford assay, and used to normalize the values. The percentage of animals with a luciferase signal above background in the respective organs is shown ($n = 50$). **c** Luciferase assay signals from all organs, and the liver as the main target organ. *Scatter graphs* representing the signal from the individual mice, and the mean are shown in LU per mg of protein. Since the liver signal from a mouse from the GemLip 8 mg/kg is out of range, the *Y*-axis is depicted segmented

bioluminescence measurements (e.g. Fig. 3c: control animal (right) day 21) were observed, but a significant growth delay induced by the treatment with 8 mg/kg GemLip treatment could be demonstrated, with an almost immediate onset of the action of the drug (Fig. 3b).

The endpoint analysis confirmed the results from the in vivo bioluminescence measurement, demonstrating a significant effect of GemLip at 8 mg/kg on the growth of the orthotopically implanted MIA PaCa-2 cells. The free Gemcitabine, as well as the 4 mg/kg GemLip treatment

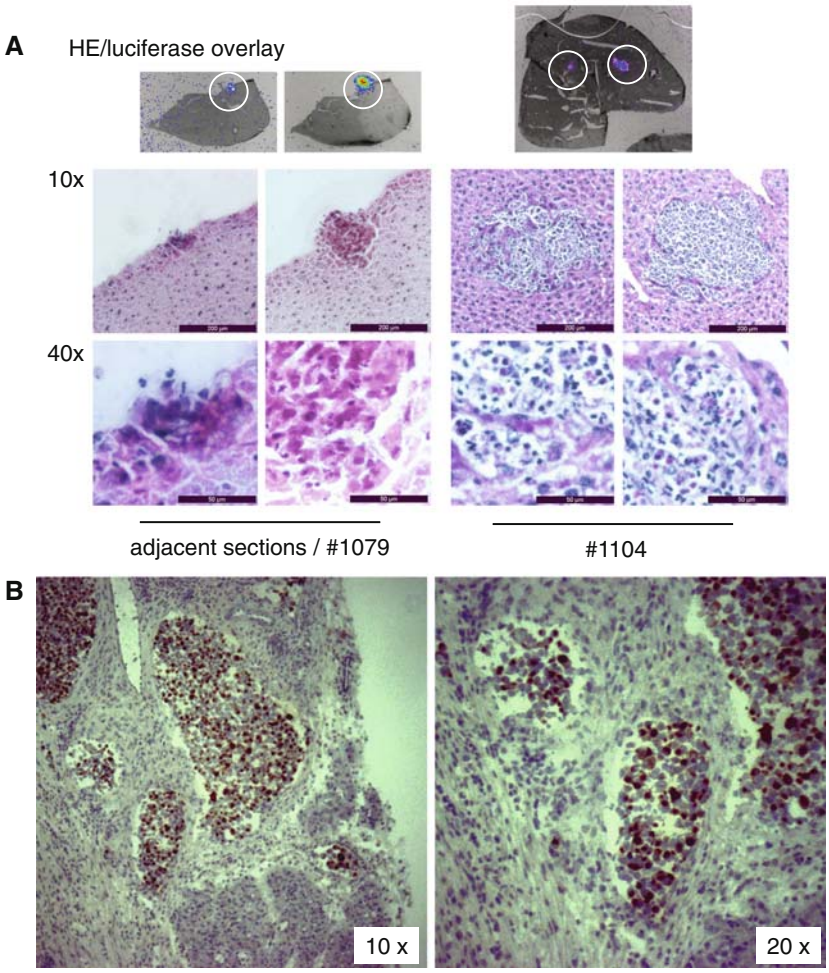

Fig. 6 Histological analysis of liver and pancreas tissue. **a** Luciferase activity measurement and subsequent HE-staining of liver sections from animals #1079 and 1104 (control group). Cryosections prepared from liver tissue were incubated with luciferin and ATP, and exposed to a CCD camera for 2 min. at 1 × 1 binning. The sections were then washed, and H&E stained. In the *upper row*, overlays are shown of the H&E stain with the luciferase signal. Underneath, 10 and 40× magnifications of the positive scoring areas are shown. In the luciferase assay, animal #1079 produced 208 LU/mg protein in the liver, #1104 2040 LU/mg protein. **b** Pan-cytokeratin (CK) 1–8 staining of the primary tumor of animal #1086 (gemcitabine group). Two magnifications of the area adjacent to normal pancreatic tissue are shown, demonstrating the infiltration of healthy tissue by MIA PaCa-2 cells. Brown are CK-positive tumor cells, blue is the hematoxylin counterstain. The other half of the pancreas scored ca. 2,500 U/mg protein when assayed for luciferase activity

group showed, at the most, a slightly reduced average tumor size (Fig. 4a, b). For the GemLip 8 mg/kg formulation, this is a very promising result, suggesting that this novel formulation of Gemcitabine does indeed have improved in vivo activity. The protection of Gemcitabine from deamination in the plasma, along with the enhanced accumulation of the small liposomes into the tumors, may both contribute to higher levels of the active Gemcitabine metabolite, dFdCTP, within the tumor cells.

Why Gemcitabine did not produce a more pronounced anti-tumoral effect may be explained by the dosage chosen and the weekly scheduling. MTD values in nude mice were 6–9 mg/kg for the earlier formulation of GemLip, and 360–480 mg/kg for Gemcitabine (Gemzar®) [8]. In a small toxicity study applying the improved GemLip formulation to the NMRI nude mice used here, the MTD for i.v. injections once a week was around 15–20 mg/kg (data not shown). In the previous report, the drugs were applied close to the MTD for 3 weeks, but considerable toxicity had been observed [8]. Due to its slow growth, the MIA PaCa-2 model allows a 5 weeks treatment scheme. In order to prevent the loss of animals, Gemcitabine was therefore applied at around 1/2 MTD (240 mg/kg), and GemLip at 1/2 MTD and 1/4 MTD (8 and 4 mg/kg, respectively), i.v. once weekly. Empty liposomes, at the dosage of the 8 mg/kg GemLip, served as a control. The chosen weekly schedule for Gemcitabine is in contrast to the reported most effective 3-days schedule at a reduced dose, 120 mg/kg [29]. Since it is not clear, whether a shorter schedule for GemLip might be effective, and tolerated, a weekly schedule was chosen here for both drugs to better compare the results.

The metastases distribution pattern, as determined via luciferase assays of a number of potential target organs, confirmed the results of previous studies [19, 20], and suggested the liver as the main site for MIA PaCa-2 metastatic dissemination (Fig. 5b). Furthermore, the high luciferase activity detected in most of the apparently healthy pancreas tissue isolates reflects infiltration by tumor cells. Tumor recurrence is a major problem in human disease [30]. In a similar orthotopic MIA PaCa-2 pancreatic mouse model, the primary tumor could only be successful resected up to

4 weeks after implantation. Two weeks later, tumor recurrence was observed in four out of five animals [31].

All treatments reduced the overall metastatic burden, as well as that of the liver, as measured via luciferase assays (Fig. 5c), except of the 8 mg/kg GemLip treatment. The elevated mean in this group is due to one animal with a heavily infiltrated liver. Two other animals of that group had heavily metastasized lungs or lymph nodes, respectively (data not shown). A stimulation of metastatic growth following a successful anti-tumor treatment or a resection of the primary tumor has been occasionally observed. Similarly, in a mouse model, re-implantation of a primary tumor resulted in suppression of metastases [32].

Surprisingly, the empty liposomes, although ineffective against the primary tumor, strongly inhibited the development of metastases, as suggested by the absence of high luciferase counts in any of the organs investigated (Fig. 5c). The absence of an effect on the primary tumor may be explained by the composition of the VPGs, which consisted mainly of hydrogenated phosphatidylcholine from egg made of C16- and C18-fatty acids with less than 1% of C14- and shorter fatty acids (GC-analytics, data not shown). In HL60 cells, dimyristoyl(C14)-phosphatidylcholine has recently been shown to induce apoptosis and dilauroyl(C12)phosphatidylcholine necrosis, whereas dipalmitoyl(C16)phosphatidylcholine showed absolutely no effect [33]. The promising anti-metastatic effect of the empty liposomes used in this study thus clearly requires further investigations on its mode of action. Since the growth of the primary tumor was not affected, however, the liposomes must have exerted an effect on metastatic signalling.

Thus, GemLip shows promising activity against primary tumor and metastases in pancreatic cancer, probably due to its protection from inactivation and the passive targeting effect mediated by the liposomes. Luciferase marked tumor cells, on the other hand, clearly proved to be a powerful tool to detect and quantify metastases, and to monitor a drug treatment in the living animal even after orthotopical implantation. The anti-tumor, and anti-metastatic activities of Gemlip, as well as the empty liposomes, will be further tested using different cell lines and mouse tumor models.

Acknowledgment We are extremely grateful to Marta Rodriguez-Franco and Gunter Neuhaus (Institute for Biology II; Cell Biology;University Freiburg) for the permission to use their CCD camera, and their lab-members for hosting us. Furthermore, we would like to thank Sandra Pöllath and Bianca Giesen for excellent technical assistance, and Lenka Taylor for critically reading the manuscript. This work was funded, in part, by grants from the Clotten Stiftung and Dietmar Hopp Stiftung GmbH.

References

1. Jemal A, Tiwari RC, Murray T, Ghafoor A, Samuels A, Ward E, Feuer EJ, Thun MJ (2004) CA Cancer J Clin 54(1):8–29
2. Noble S, Goa KL (1997) Drugs 54(3):447–472
3. Axelson J, Lindell M, Horlin K, Ohlsson B (2005) Pancreatology 5(2–3):251–258
4. Zagon IS, Jaglowski JR, Verderame MF, Smith JP, Leure-Dupree AE, McLaughlin PJ (2005) Cancer Chemother Pharmacol 56(5):510–520
5. Abbruzzese JL, Grunewald R, Weeks EA, Gravel D, Adams T, Nowak B, Mineishi S, Tarassoff P, Satterlee W, Raber MN et al (1991) J Clin Oncol 9(3):491–498
6. Wang LR, Huang MZ, Xu N, Shentu JZ, Liu J, Cai J (2005) J Zhejiang Univ Sci B 6(5):446–450
7. Reid JM, Qu W, Safgren SL, Ames MM, Krailo MD, Seibel NL, Kuttesch J, Holcenberg J (2004) J Clin Oncol 22(12):2445–2451
8. Moog R, Burger AM, Brandl M, Schuler J, Schubert R, Unger C, Fiebig HH, Massing U (2002) Cancer Chemother Pharmacol 49(5):356–366
9. Shipley LA, Brown TJ, Cornpropst JD, Hamilton M, Daniels WD, Culp HW (1992) Drug Metab Dispos 20(6):849–855
10. van Borssum Waalkes M, Kuipers F, Havinga R, Scherphof GL (1993) Biochim Biophys Acta 1176(1–2):43–50
11. van Borssum Waalkes M, van Galen M, Morselt H, Sternberg B, Scherphof GL (1993) Biochim Biophys Acta 1148(1):161–172
12. Yuan F, Dellian M, Fukumura D, Leunig M, Berk DA, Torchilin VP, Jain RK (1995) Cancer Res 55(17):3752–3756
13. Massing U (1997) Int J Clin Pharmacol Ther 35(2):87–90
14. Massing U, Fuxius S (2000) Drug Resist Updat 3(3):171–177
15. Brandl M, Massing U (2003) Vesicular phospholipid gels. In: New RW, Torchillin V (eds) Liposomes practical approaches. IRL-Press at Oxford University Press, Oxford
16. Schueler J (1998) Entwicklung und Charakterisierung humaner Tumormodelle durch orthotope Implantation. In: Inst. für Veterinärpathologie, Freie Universität, Berlin
17. Sipos B, Moser S, Kalthoff H, Torok V, Lohr M, Kloppel G (2003) Virchows Arch 442(5):444–452
18. Bold RJ, Chandra J, McConkey DJ (1999) Ann Surg Oncol 6(3):279–285
19. Katz MH, Bouvet M, Takimoto S, Spivack D, Moossa AR, Hoffman RM (2003) Cancer Res 63(17):5521–5525
20. Hotz HG, Reber HA, Hotz B, Yu T, Foitzik T, Buhr HJ, Cortina G, Hines OJ (2003) Pancreas 26(4):e89–e98
21. Tomioka D, Maehara N, Kuba K, Mizumoto K, Tanaka M, Matsumoto K, Nakamura T (2001) Cancer Res 61(20):7518–7524
22. Tsutsumi S, Yanagawa T, Shimura T, Kuwano H, Raz A (2004) Clin Cancer Res 10(22):7775–7784
23. Bouvet M, Yang M, Nardin S, Wang X, Jiang P, Baranov E, Moossa AR, Hoffman RM (2000) Clin Exp Metastasis 18(3):213–218
24. Shah K, Weissleder R (2005) NeuroRx 2(2):215–225
25. Tardi C (1999) Vesikuläre Phospholipidgele: in vitro Charakterisierung, Autoklavierbarkeit, Anwendung als Depotarzneiform. In. Dept. Pharmaceutical Technology, Albert-Ludwigs-University of Freiburg, Freiburg
26. Gossen M, Bujard H (1992) Proc Natl Acad Sci USA 89(12):5547–5551
27. Workman P, Balmain A, Hickman JA, McNally NJ, Rohas AM, Mitchison NA, Pierrepoint CG, Raymond R, Rowlatt C, Stephens TC et al (1988) Lab Anim 22(3):195–201
28. Giovannetti E, Mey V, Danesi R, Mosca I, Del Tacca M (2004) Clin Cancer Res 10(9):2936–2943
29. Braakhuis BJ, van Dongen GA, Vermorken JB, Snow GB (1991) Cancer Res 51(1):211–214
30. Sener SF, Fremgen A, Menck HR, Winchester DP (1999) J Am Coll Surg 189(1):1–7
31. Eibl G, Reber HA (2005) Pancreas 31(3):258–262
32. Keller R (1985) Invasion Metastasis 5(5):295–308
33. Nagami H, Nakano K, Ichihara H, Matsumoto Y, Ueoka R (2006) Bioorg Med Chem Lett 16(4):782–785